Petrology and Geochemistry of El Chichón and Tacaná: Two Active, yet Contrasting Mexican Volcanoes

2

José Luis Arce, James Walker, and John Duncan Keppie

Abstract

El Chichón and Tacaná have been widely considered subduction-related volcanoes, although they show differences in mineral assemblage and magma composition. El Chichón emitted potassium- and sulfur-rich trachyandesites and trachybasalts during its eruptive history, whereas Tacaná erupted basalts to dacites with moderate potassium contents, and minor high-Ti magmas. The magmatic evolution in both volcanoes involved similar fractionating assemblages of Fe-Ti oxides, olivine, plagioclase, pyroxenes, amphibole and apatite. Both K_2O/P_2O_5 ratios and isotopic signatures, indicate that the melts of El Chichón and Tacaná experienced significant crustal contamination. Magma genesis for both volcanoes has been related to the northeastward subduction of the Cocos Plate. Even if such origin agrees with the location of Tacaná, situated 100 km above the Cocos Benioff Zone, a subduction origin is at odds with recent tectonic and geophysical data obtained for southern Mexico for El Chichón, located about 400 km from the trench. In this chapter we review the existing petrographic and geochemical data for El Chichón and Tacaná volcanoes, in order to understand their magma genesis and evolution.

Keywords

Tacaná and El Chichón volcanoes · Petrology and geochemistry · Potassium-rich magmas

2.1 Introduction

Volcanism occurs at several tectonic environments, including subduction, rift, and hot spot regions, and magma genesis is controlled mainly by three factors: temperature, pressure, and the presence of volatiles (Schmincke 2004). Petrological and geochemical data, including isotopic ratios, and trace element concentrations, can be fingerprints of the volcano-tectonic environment (Best 2003). Subduction-related magmas are distinctively enriched in large-ion-lithophile elements (LILE), and depleted in high-field-strength elements

J.L. Arce (✉) · J.D. Keppie
Instituto de Geología, Cd. Universitaria Coyoacan, UNAM, 04510 Coyoacan, Mexico
e-mail: jlarce@geologia.unam.mx

J. Walker
Department of Geology and Environmental Geosciences, Northern Illinois University, DeKalb, IL, USA

T. Scolamacchia and J.L. Macías (eds.), *Active Volcanoes of Chiapas (Mexico): El Chichón and Tacaná*, Active Volcanoes of the World, DOI 10.1007/978-3-642-25890-9_2,

(HFSE) relative to Mid-Ocean Ridge Basalts (MORB) magmas (Tatsumi and Kogiso 1997). These features have been attributed to fluid fluxes deriving from the subducted slab (Saunders et al. 1980), although in tectonically complex subduction zones, magma chemistry may reflect the added tectonic complexity (Gazel et al. 2009) (i.e. the presence of the Tehuantepec Ridge and the Polochic-Motagua fault zone, in southern Mexico).

Both El Chichón and Tacaná volcanoes have been related to the subduction of the Cocos plate beneath the North America plate (Luhr et al. 1984; Mora et al. 2004; Chap. 1). Nevertheless the presence of the Tehuantepec ridge (Fig. 2.1), a prominent lithospheric structure in the Cocos plate, which could extend below El Chichón (Luhr et al. 1984; Manea et al. 2005), complicates the tectonic framework of the area.

Tacaná (4,050 masl) represents the northernmost volcano of the Central American Volcanic Arc (CAVA) (Mercado and Rose 1992; Mora et al. 2004; García-Palomo et al. 2006). El Chichón (1,100 masl) is the youngest structure of the NW-trending Modern Chiapanecan Volcanic Arc (MCVA of Damon and Montesinos 1978), which includes ten volcanoes (Mora et al. 2007) varying in age from 2.2–0.4 Ma (see Chap. 1).

The NW-trending, 150 km long MCVA has been related to the subduction of the Cocos Plate beneath the North American Plate (Damon and Montesinos 1978) and it is located at a distance of approximately 300–400 km from the Middle America Trench (MAT). The Cocos Plate beneath the volcano reaches a depth of about 200 km, with a dip of 40–45º (Rebollar et al. 1999; Manea and Manea 2006).

El Chichón consists of pyroclastic materials, lava domes and other volcanic edifices (see Chap. 3 for stratigraphic details). Both lava domes and pyroclastic material have a uniform composition of alkaline rocks, ranging between K-rich trachyandesitic and trachydacitic rocks (Luhr et al. 1984; McGee et al. 1987; Macías et al. 2003). One of the most important characteristics of the 1982 El Chichón eruption was the great sulfur content of its magma (2.6 wt% SO_3; Luhr et al. 1984). Evidence for such high content was the generation of anhydrite crystals recognized for the first

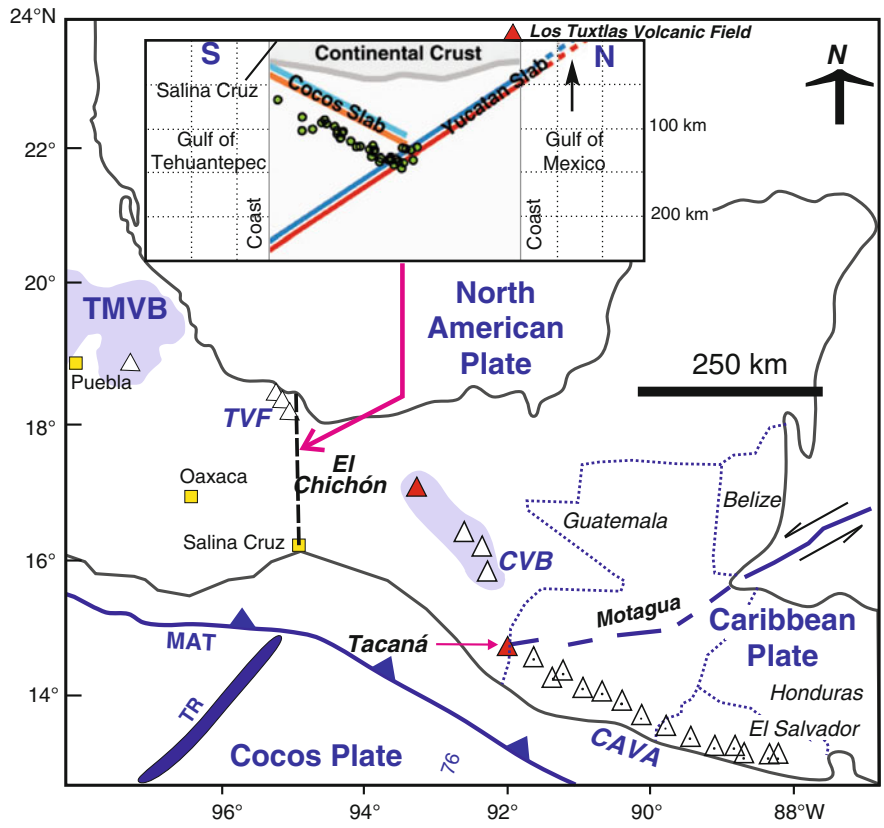

Fig. 2.1 Location map of the El Chichón and Tacaná volcanoes in southern Mexico. *TMVB* Trans-Mexican Volcanic Belt; *CAVA* Central American Volcanic Arc; *CVB* Chiapanecan Volcanic Belt; *MAT* Middle American Trench; *TR* Tehuantepec Ridge. *Inset* is a model showing interaction of the Cocos and Yucatán slabs underneath El Chichón and the Los Tuxtlas Volcanic Field (LTVF) (after Kim et al. 2011)

time in pumice samples of the 1982 eruption. Fresh pumice samples contained up to 2 wt% suhedral to euhedral, anhydrite crystals, in association with hornblende, biotite, and sphene phenocrysts (Luhr et al. 1984). Moreover, the trachyandesites emitted in 1982 were rich in K, Rb, Sr, Th, U, and Cs, compared to other Mexican and Central American volcanoes, fact that was attributed to the relatively large distance from the Middle America Trench (Luhr et al. 1984) (Fig. 2.1). Alkaline rocks in subduction zones have been linked to the presence of fracture zones (DeLong et al. 1975). At El Chichón, such assumption would be consistent with the presence of the Tehuantepec ridge underneath this volcano (Fig. 2.1).

Recent seismic data (Kim et al. 2011) obtained by teleseismic P-to-S converted waves suggest an anomalous southwest-dipping slab in southern Mexico. This interpretation would indicate that the Cocos plate does not directly underlie El Chichón, implying that El Chichón lies just to the south of a projection of the intra-Yucatán subduction zone. Such zone would be a southwest-dipping structure active during the Miocene, which generated a slab descending up to 250 km depth (Kim et al. 2011), truncating the Cocos slab at circa 100 km depth (Fig. 2.1). At a local scale, El Chichón is situated inside a sinistral E-W fault system (San Juan Fault System of García-Palomo et al. 2004; Chap. 1).

Tacaná is a typical stratovolcano with steep slopes that belongs to the Tacaná Volcanic Complex (TVC, see Chaps. 1 and 6). It is composed of calc-alkaline, andesitic to dacitic lava flows, and pyroclastic deposits of similar compositions (Mercado and Rose 1992; Mora et al. 2004; García-Palomo et al. 2006). It lies on the trace of the sinistral Polochic-Motagua Fault zone, which according to Guzman-Speziale et al. (1989) represents the boundary between the North American and Caribbean plates in Guatemala and southern Mexico. The TVC is located ~200 km from the MAT, and approximately 100 km above the subducting Cocos slab which dips about 40º (Rebollar et al. 1999; Syracuse and Abers 2006). The magmatism that generated the CAVA volcanism has been focus of numerous investigations (i.e. Carr et al. 1990; Feigenson and Carr 1993; Carr et al. 2003; Abers et al. 2003; Bolge et al. 2009). Despite the clear relationship of the CAVA with the Cocos plate subduction, large variations in trace elements and isotopic ratios have been reported at regional level (Carr et al. 1990; Bolge et al. 2009), and explained with variations in slab depths, slab inputs, crustal architecture, and tectonic segmentation (Carr et al. 1990; Patino et al. 2000; Bolge et al. 2009).

In this chapter we present the current knowledge of petrological aspects of El Chichón and Tacaná active volcanoes, concerning to their magmatic evolution and present the ideas about the genesis of their magmas, based on published whole-rock chemistry, isotope data, and petrological information.

2.2 Petrography and Geochemistry

2.2.1 El Chichón

Several petrological and geochemical studies have been carried out at El Chichón since the 1982 eruption. Initial investigations indicated the presence of subhedral phenocrysts of anhydrite in fresh ejecta (Luhr et al. 1984). Subsequent petrological and geochemical works reported that not only the 1982 magma, but also the magmas erupted before 1982 were sulfur-rich (Rose et al. 1984; McGee et al. 1987). Rose et al. (1984) analyzed undefined lava dome and pyroclastic flow deposits, outcropping inside the inner 1982 crater walls, consisting of porphyritic trachyandesites, with a crystallinity ranging from 20 to 40 vol% (Rose et al. 1984). Pumice samples of the 1982 eruption (unit A, see Chap. 3) are also porphyritic and vesicular, with crystallinity between 19 and 29 vol% (Luhr et al. 1984) characterized by abundant, and large (0.3–4 mm) phenocrysts of plagioclase and amphibole. Pumice samples from the fallout deposit of Unit B (Chap. 3) show a porphyritic texture (Fig. 2.2a) with up to 20 vol% crystals of plagioclase (6–12 vol %) + amphibole + clinopyroxene + Fe-Ti oxides, set in a groundmass (25–36 vol%) of microlites and glass (Macías et al. 2003). Plagioclase crystals are euhedral to anhedral (Fig. 2.2a, b), mostly showing normal zonation, and have compositions varying from An_{46} to An_{65} in the cores to An_{35} to An_{40} in the rims. The reverse zoning observed in some cases (i.e. An_{41} in the core and An_{47} in the rim) was interpreted as a result of repeated and continuous recharge episodes by relatively mafic magmas (Macías et al. 2003). In Unit B, hornblende represents ~2 vol% with a homogeneous compositions of magnesian hastingsite and minor tschermakite (Macías et al. 2003). Augite and Fe-Ti

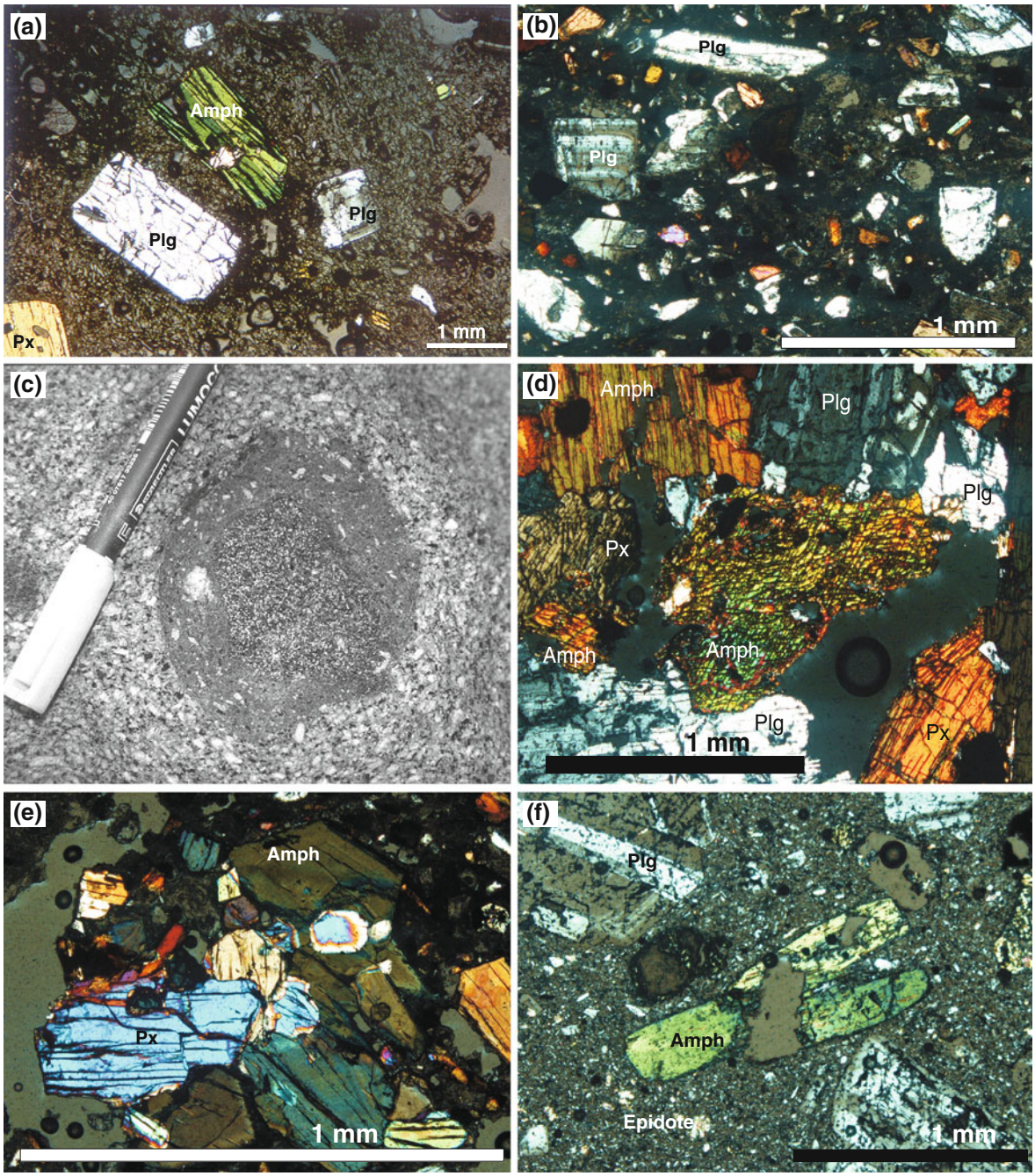

Fig. 2.2 **a** Cross-polarized microphotograph of Unit B pumice sample, showing a porphyritic texture, with phenocrysts of plagioclase (*Plg*), pyroxene (*Px*), amphibole (*Amph*), Fe-Ti oxides (*oxi*) in a groundmass and vesicular matrix (After Macías et al. 2003); **b** Cambac dome sample showing typical porphyritic textures, with abundant plagioclase, pyroxene and amphibole phenocrysts; **c** Mafic enclave in trachyandesitic lava domes (Somma domes) at the head of the Agua Tibia valley. Rounded enclaves commonly show assimilation aureoles, containing abundant plagioclase phenocrysts. The marker is 14 cm long (After Macías et al. 2003); **d** Representative cross-polarized microphotographs of mafic enclaves (CH-ME) found in El Chichón samples, and showing equigranular textures containing plagioclase (*Plg*) pyroxene (*Px*), amphibole (*Amph*), and Fe-Ti oxides (After Arce et al. 2014); microphotographs from **e** Cambac and **f** Capulín dome samples

oxides occur in minor amounts (<1 vol%) (Macías et al. 2003).

Pumice and dense lithic samples from units C, D, E, F, and J (Chap. 3) show similar petrographic characteristics, with a porphyritic texture consisting of phenocrysts and microphenocrysts of plagioclase + amphibole + clinopyroxene ± Fe-Ti oxides (11–42 vol% of crystals). Even if always with euhedral rims, plagioclase crystals show different internal textures, such as sieved and patchy zones, interpreted to have formed during multiple recharge events inside the magma chamber (Andrews et al. 2008). Accessory minerals in every sample include magnetite, apatite, and titanite, whereas biotite is present only in samples of Unit D (1,250 year BP eruption), in which clinopyroxene is absent (Andrews et al. 2008).

Samples from the Capulín, NW, SW and Cambac lava domes, (see Chap. 3 for their location) included numerous mafic enclaves (Espíndola et al. 2000; Macías et al. 2003, 2010a; Arce et al. 2014). The mafic enclaves show an equigranular texture (Fig. 2.2c, d), with a mineral assemblage consisting of amphibole + augite + enstatite + plagioclase + olivine, and minor Fe-Ti oxides (Espíndola et al. 2000; Macías et al. 2003). The lava dome samples are highly crystalline (up to 60 vol%), with a mineral assemblage (in order of abundance) of plagioclase, amphibole, clinopyroxene, ilmenite, titanomagnetite, apatite and sometimes biotite (Fig. 2.2b–f). Apatite is more common as inclusions in plagioclase crystals (Macías et al. 2010a). The presence of anhedral epidote in dome samples matrix was interpreted as a product of hydrothermal activity (Arce et al. 2014).

As mentioned before, primary igneous anhydrite was described for the first time worldwide in the trachyandesitic pumice erupted in 1982 (Luhr et al. 1984), commonly associated with crystals of apatite (Luhr 2008). Given the similar chemistry of the rocks emitted during El Chichón history (see below), magmatic anhydrite was with all probabilities a characteristic feature of its products, even if rarely found in its rocks due to meteoric alteration. In fact Luhr et al. (1984), pointed out that after a single rainy season at El Chichón, the anhydrite in pumice samples was dissolved. Notably, primary anhydrite has been also reported in other volcanoes in the Chiapanecan Volcanic Arc, (i.e. La Lanza and Venustiano Carranza domes located close to San Cristobal de las Casas; Luhr 2008). In summary, all volcanoes of the Chiapanecan Volcanic Arc seem to share similar mineral assemblages and whole-rock chemistry (Mora et al. 2010).

Plagioclase crystals in lava and pumice samples (lava domes and pyroclastic deposits) among different units (i.e. A, B, C, D) show a wide variety of textural features, such as complex compositional zonation, sieve textures, and corroded margins (Fig. 2.2b), all of which have been interpreted as the result of multiple recharge events from deeper and hotter magmas entering in a subvolcanic magma chamber operative throughout the entire history of the volcano (Tepley et al. 2000; Andrews et al. 2008; Macías et al. 2003). Mafic enclaves found in lava domes and pyroclastic deposits (Macías et al. 2003; Layer et al. 2009; Arce et al. 2014) represent another evidence of injections of mafic magmas and mixing as well.

The whole-rock chemistry of El Chichón samples (Luhr et al. 1984; McGee et al. 1987; Espíndola et al. 2000; Macías et al. 2003; Andrews et al. 2008; Layer et al. 2009) has been grouped according to sample ages "or associated structures" into: 1982 eruption, Holocene, Pleistocene, Dome structures, mafic enclaves, and Chapultenango trachybasalt (Arce et al. 2014).

The lava domes and pyroclastic deposits sampled inside the 1982 crater, with trachyandesitic composition (54.5–58 wt% SiO_2) belong to the Holocene group, based on their stratigraphic position and according to Rose et al. (1984) these rocks would be slightly lower in SiO_2, Na_2O, K_2O with respect to the 1982 products. Nevertheless, Layer et al. (2009) did not find a clear temporal correlation with rock composition (Fig. 2.3).

The whole rock pumice samples from 1982 eruption are characterized by similar SiO_2 contents (55–58 wt%) compared to other units of the Holocene, and Pleistocene groups (Espíndola et al. 2000; Andrews et al. 2008). In contrast, samples from the domes (Cambac, Capulin, NW and SW domes) apparently show a broader variation in SiO_2 contents (52–60 wt %) (McGee et al. 1987; Espíndola et al. 2000; Layer et al. 2009; Rose et al. 1984; Arce et al. 2014) (Fig. 2.3). Up today, the few whole-rock chemical data existing for the mafic enclaves show a wide compositional range (44.5–50.5 wt% SiO_2) being mainly trachybasalts (Fig. 2.3a–j) with high contents of K_2O (Macías et al. 2003; Espíndola et al. 2000; Layer et al. 2009; Arce et al. 2014). The most mafic product of the area is the Chapultenango trachybasalt (Espíndola et al. 2000; Layer et al. 2009, see Chap. 3).

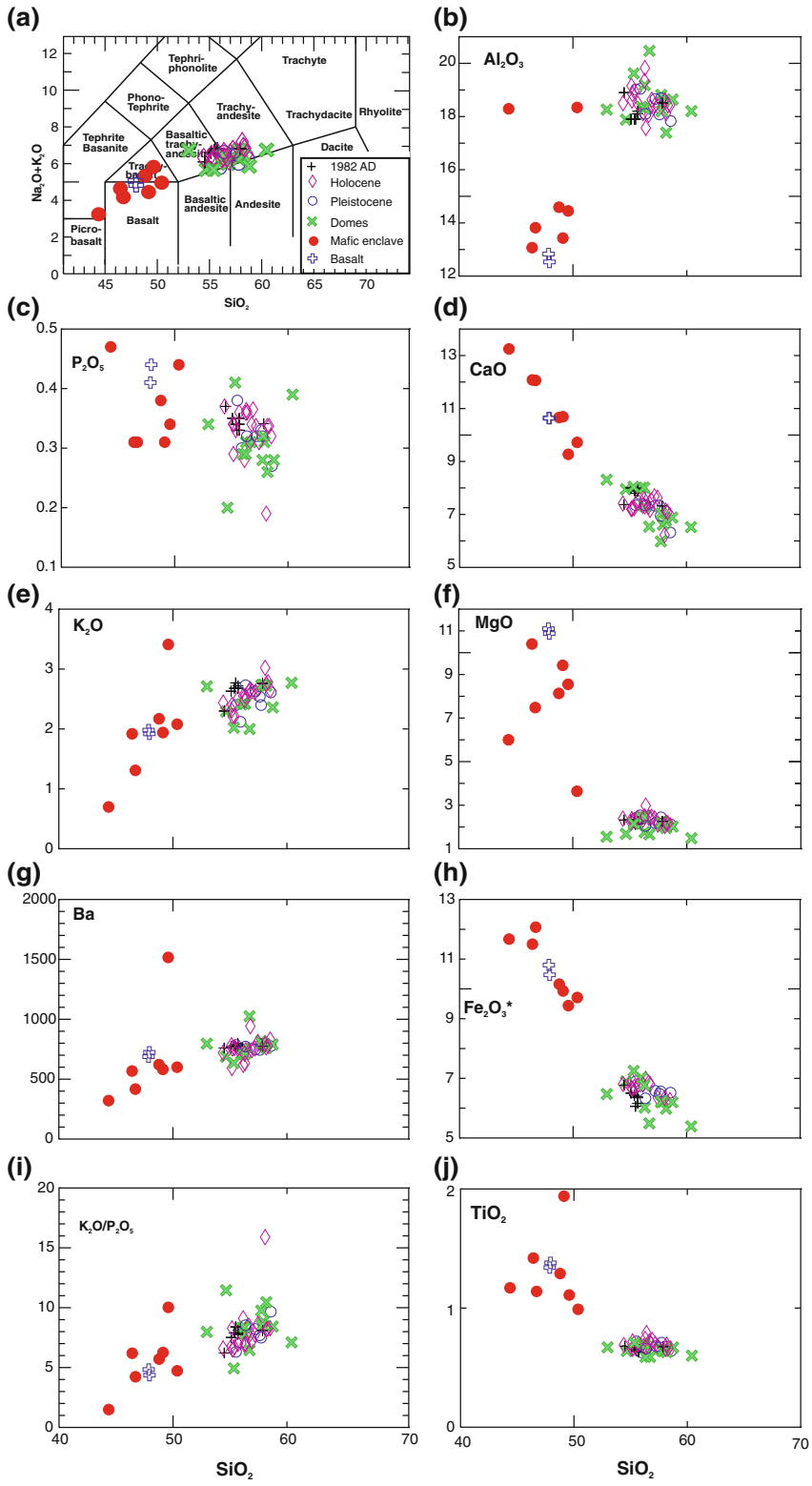

Fig. 2.3 **a** Total alkalies versus silica diagram (Le Bas et al. 1986), of El Chichón samples; **b–j** Harker diagrams. Major elements in wt% (recalculated on anhydrous basis) and trace elements in parts per million (ppm). Data taken from Luhr et al. (1984), Rose et al. (1984), McGee et al. (1987), Espíndola et al. (2000), Macías et al. (2003), Andrews et al. (2008), Layer et al. (2009) and Arce et al. (2014)

In general, all El Chichón samples are K-rich, and some unusually P-rich (Fig. 2.3), particularly some trachybasalts and trachyandesites. Harker diagrams (Fig. 2.3b–j) show that the more mafic compositions (i.e. trachybasalts) could represent the parental compositions for the more evolved trachyandesites erupted at El Chichón. Mafic enclaves are often interpreted as the product of magma mixing (Eichelberger et al. 1976; Stimac and Pierce 1992). The enclaves display a broadly linear array on Harker diagrams, consistent with a mixing relationship for compositions intermediate between parental trachybasalts and more evolved trachyandesites. Some mafic enclaves however, do not lie on simple mixing lines and therefore could indicate a more complex origin (Browne et al. 2006). On an Al_2O_3 versus SiO_2 diagram a notable inflection exists (Fig. 2.3b) explained as indicative of a change from an early plagioclase-poor to a later, plagioclase-rich assemblage (Arce et al. 2014). The steadfast declines in Fe_2O_3 and TiO_2 on Harker plots would attest an early fractionation of either Fe-Ti oxides, or amphibole, and the development of a calc-alkaline trend (Arce et al. 2014; Fig. 2.3h, j). Similarly, decreasing P_2O_5 concentrations during differentiation would

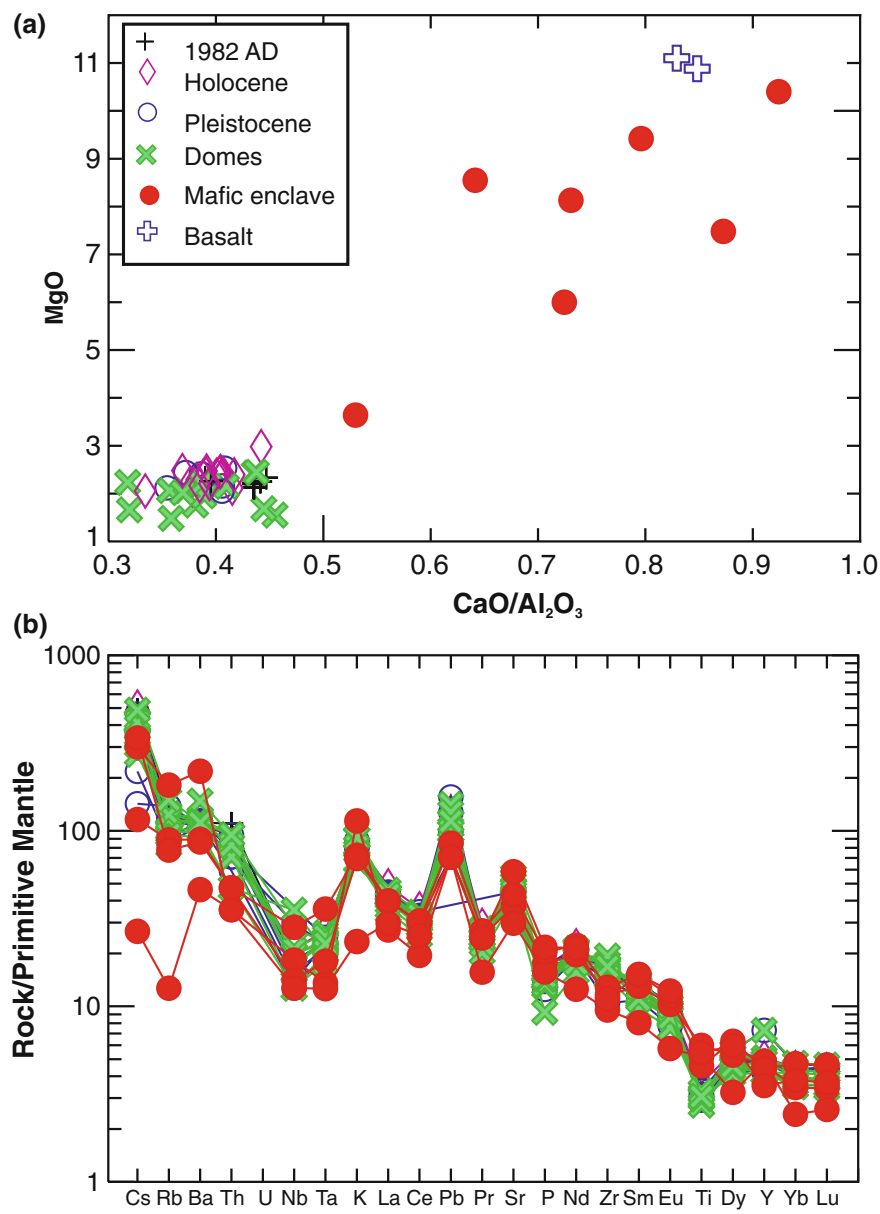

Fig. 2.4 **a** MgO versus CaO/Al_2O_3 ratio for El Chichón samples. All samples were recalculated to 100 % on an anhydrous basis; **b** Spider diagram of selected El Chichón samples, normalized to primitive mantle (Sun and McDonough 1989). Data taken from Arce et al. (2014)

require an early saturation with apatite (Arce et al. 2014; Fig. 2.3c). The decline of the CaO/Al_2O_3 ratio with MgO (Fig. 2.4a) also strongly suggests that early fractionation in the El Chichón magmatic system is dominated by the removal of clinopyroxene (i.e. Walker 1981).

In the Harker diagrams (Fig. 2.3b–j) two geochemical groups are observed with contrasting TiO_2, MgO, Fe_2O_3, Al_2O_3 contents that also have conspicuously different K_2O/P_2O_5 ratios (Fig. 2.3i), likely related by either fractional crystallization, or contamination and magma mixing (Arce et al. 2014). One of the most characteristic features of El Chichón is the production of trachyandesitic anhydrite-bearing magmas, enriched in potassium and sulphur, throughout its active period (Rose et al. 1984; Luhr 2008).

Trace elements in volcanic rocks tend to fractionate into specific minerals and therefore are useful in formulating models for magmatic differentiation and, in some cases, predicting the magma source (Winter 2001). Trace elements in El Chichón volcanic rocks are relatively depleted in Nb, Ta, and Ti, and relatively enriched in LILE, particularly Pb with respect to other trace elements (Fig. 2.4a, b). Such behavior would indicate a subduction related magmatism, involving the subducted slab, either melts or just fluids from it.

Both trachybasalts (i.e. Chapultenango basalt) and trachyandesites (dome samples, and pumice) show similar trace element patterns. The mafic rocks have generally lower concentrations of most incompatible elements (i.e. Ti, Y, Yb, Lu) (Fig. 2.4b), with the notable exceptions of P, as pointed out above. Some high-Ti samples (mafic enclaves) do not show enrichments in other high field strength elements (i.e. Zr, Nb, Ta, Th, U) (Fig. 2.4b) as would have been expected in mafic melts.

Only few $^{87}Sr/^{86}Sr$ and $^{143}Nd/^{144}Nd$ isotopic ratios have been published (Macías et al. 2003; Andrews et al. 2008) for El Chichón volcanic rocks (Fig. 2.5). Values of $^{87}Sr/^{86}Sr$ range from 0.70406 to 0.70426 and $^{143}Nd/^{144}Nd$ from 0.51273 to 0.51279 and are distinctively more radiogenic compared to most Central American Volcanic Arc rocks, but only overlap those ratios of some lavas from Guatemala volcanoes (i.e. Tajumulco volcano, Tacaná's nearest volcanic neighbor in northwestern Guatemala). $^{87}Sr/^{86}Sr$ ratios in plagioclase crystals from Holocene deposits (Tepley et al. 2000; Andrews et al. 2008) show a complex correlation with An contents. Such results have been interpreted with the occurrence of multiple recharge events of a hot magma with low $^{87}Sr/^{86}Sr$ ratios, and high Sr contents, that eventually homogenize with a cooler magma to produce a hybrid magma. The assimilation of sedimentary rocks with high $^{87}Sr/^{86}Sr$ ratios, by El Chichón magmas has been also proposed to explain the complex isotopic zonation in plagioclase crystals (Tepley et al. 2000; Andrews et al. 2008).

2.2.2 Tacaná

The Tacaná Volcanic Complex (TVC) consists of four aligned structures Chichuj, Tacaná, Las Ardillas, and San Antonio (see Chap. 6). All erupted products vary in composition from andesite to dacite (Mora et al. 2004; García-Palomo et al. 2006). Mercado and Rose (1992) were the first to describe the petrographic and geochemical characteristics of TVC rocks. They analyzed sixteen samples of lava and pyroclastic material from different deposits, obtaining compositions between 58 and 64 wt% SiO_2. Nevertheless, no radiometric ages were provided. Macías et al. (2000) published data on eight samples from San Antonio volcano; such samples included the Mixcun block-and-ash flow deposit (see Chap. 6), undifferentiated lava flows (including one mafic enclave), and domes yielding a larger compositional range from 50 to 64 wt % SiO_2. Petrographic descriptions combined with whole-rock chemical analyses of sixty samples, belonging to Chichuj, Tacaná, and San Antonio edifices, including a mafic enclave hosted in andesitic lava from San Antonio volcano were published by Mora et al. (2004). The authors obtained similar compositions (56–64 wt% SiO_2) as Macías et al. (2000) for the entire volcanic complex. A geological map of the TVC area, and the individuation of four volcanic edifices of the TVC was published by García-Palomo et al. (2006) (see Chap. 6). These authors included some general petrographic descriptions and whole-rock chemical analysis of Las Ardillas dome. More recent studies are those published by Macías et al. (2010b) who studied a debris avalanche deposit and its petrographic and geochemical characteristics, and Arce et al. (2012) who studied the eruptive dynamics and the petrology of the Sibinal Pumice deposit, produced by a Plinian eruption around 23, 540 year BP (see Chap. 6).

The rocks of the TVC were grouped according to the volcanic structure they belong to, in: Chichuj (volcano),

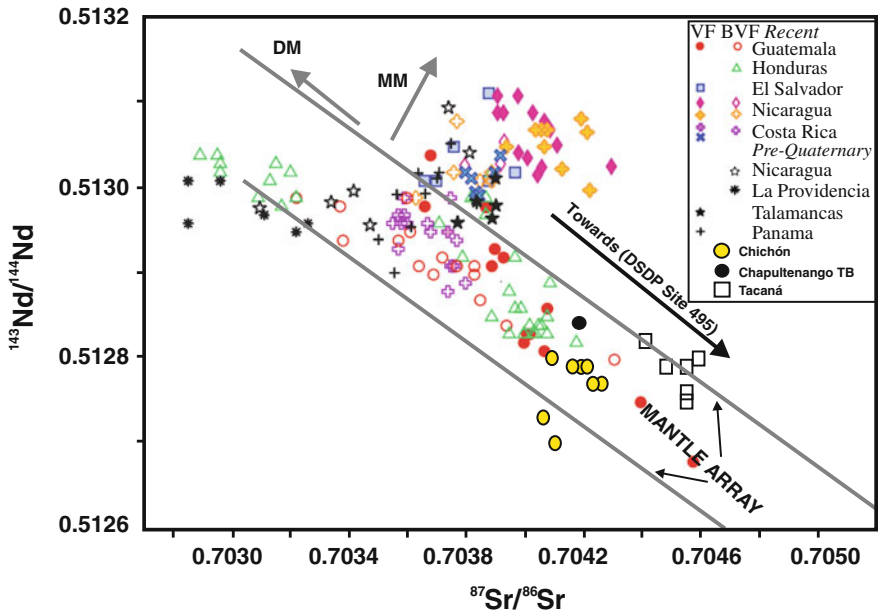

Fig. 2.5 $^{143}Nd/^{144}Nd$ versus $^{87}Sr/^{86}Sr$ ratios of El Chichón and Tacaná samples (data from Macías et al. 2003; Mora et al. 2004; Andrews et al. 2008), compared to other Central American Volcanic Arc volcanoes. *DM* depleted mantle; *MM* modified mantle. Isotopic data from CAVA volcanoes were taken from Carr et al. (1990). *DSDP Site 495* refers to hemipelagic sediments from drill Site 495 (von Huene et al. 1980)

Tacaná (volcano), Las Ardillas (dome), and San Antonio (volcano). Each group consisting of lavas and pyroclastic deposits, and mafic enclaves found into lava flows (Mora et al. 2004). Some pumice-rich pyroclastic deposits (i.e. pumice air fall and pyroclastic flow deposits) ejected from the TVC, (i.e. La Vega Pyroclastic flow (LVPF), Sibinal Pumice (SP), and Tacaná Pumice (Arce et al. 2012; Chap. 6) have been grouped separately because their source or vents (i.e. Chichuj, Tacaná, San Antonio volcanic structures) are unknown.

All of TVC rocks display a porphyritic texture, sometimes with seriate and glomeroporphyritic textures (Fig. 2.6) with crystallinity around 32 vol% (Macías et al. 2000; Mora et al. 2004). The mineral assemblage for all TVC structures is, in order of abundance, plagioclase, hornblende, clinopyroxene, orthopyroxene, ± Fe-Ti oxides (Fig. 2.6a–f), set in a glassy and sometimes microlitic matrix. Some lavas from the Tacaná edifice show trachytic textures (oriented plagioclase crystals), commonly developed during the emplacement of lava flows. Mafic enclaves show an intersertal porphyritic texture, but with crystal contents up to 65 vol% (Mora et al. 2004), and a mineral assemblage of plagioclase + hornblende + clinopyroxene + orthopyroxene + olivine, and ± Fe-Ti oxides set in a brown glass matrix (Mora et al. 2004). Olivine phenocrysts were only observed in a basaltic andesite lava flow, located just to the east of Tacana's summit (see Chap. 6). The textures of phenocrysts are quite variable in all of TVC samples, with coexisting subhedral and euhedral phenocrysts (Macías et al. 2000; Mora et al. 2004). Plagioclases exhibit complex compositional zonation and sieve textures (Fig. 2.6a, d, and e). The compositional ranges are similar: anorthite contents in Chichuj samples vary from An_{47} to An_{70} (andesine to labradorite), while San Antonio samples show a range from An_{40} to An_{84}. Plagioclase in mafic enclaves is slightly more anorthitic varying from An_{48} to An_{88} (Macías et al. 2000; Mora et al. 2004). Clinopyroxene and orthopyroxene are ubiquitous in the TVC samples, and have been classified as augite and enstatite. Amphiboles are Ca-rich, and are classified as magnesium-hornblende (Mora et al. 2004). Fe-Ti oxides are represented by titanomagnetite and lesser amounts of ilmenite (Mora et al. 2004).

Pumice samples from three main pyroclastic deposits of the TVC (i.e. La Vega Pyroclastic flow –LVPF-, Sibinal Pumice fall deposit –SP- and Tacaná Pumice fall deposit –TP-, see Chap. 6 for stratigraphic details) display porphyritic and vesicular textures (Fig. 2.6f), with a common mineral assemblage of plagioclase, clinopyroxene, orthopyroxene, Fe-Ti oxides, and minor amphibole (Arce et al. 2012).

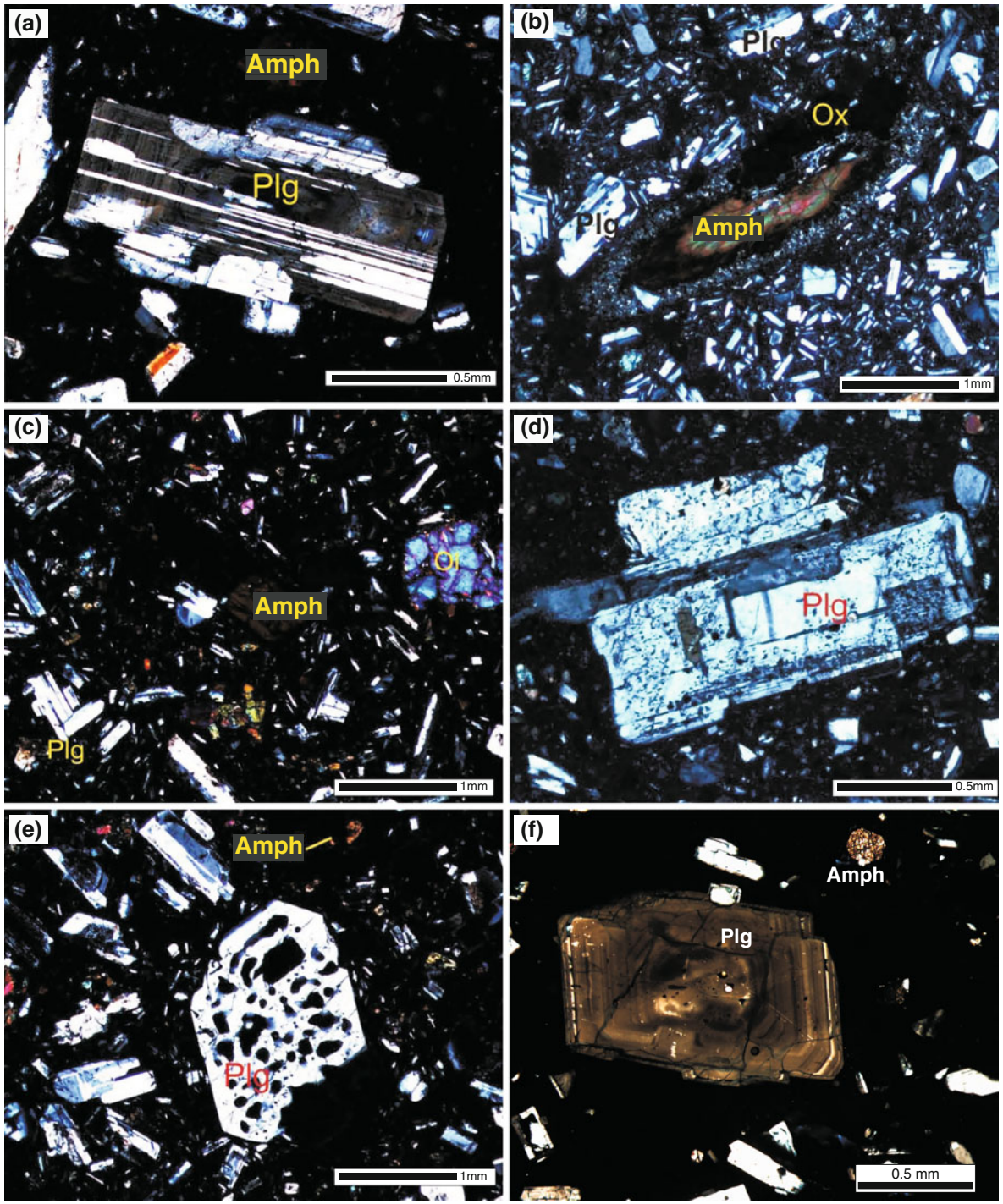

Fig. 2.6 **a**–**e** Representative cross-polarized microphotographs of Tacaná lava flow samples showing common porphyritic textures, and mineral assemblages (after Arce et al. 2014). *Amph* amphibole; *Plg* plagioclase; *Ol* olivine; *Ox* Fe-Ti oxides. Notice the different textures in plagioclase and amphibole phenocrysts. **f** Cross-polarized microphotograph of the Sibinal Pumice deposit, showing euhedral and zoned plagioclase phenocrysts. *Plg* plagioclase; *Amph* amphibole; *Cpx* clinopyroxene (after Arce et al. 2012)

Plagioclase is the most abundant mineral phase in all pumice samples, often with complex zonation (Mora et al. 2004). Anorthite contents commonly vary from An_{67} to An_{42} for the Sibinal Pumice and Tacaná Pumice deposits (Arce et al. 2008), whereas for the La Vega pyroclastic flow deposit, a wider range is recorded (An_{75}–An_{45}).

Clinopyroxene (diopside) and orthopyroxene (hypersthene) are also abundant in pumice deposits and compositionally homogenous (Arce et al. 2012). They are subhedral to euhedral, and in some samples exhibit reaction rims composed of amphibole and plagioclase. Amphibole phenocrysts are subhedral to anhedral, sometimes with a reaction rim (coronae surrounding the crystals) made of Fe-Ti oxides (Fig. 2.6b) suggesting changes in the ascent velocity during the eruption (Browne and Gardner 2006), or simply oxidation of the amphibole.

Although there are robust whole-rock chemical data sets for the TVC, only few include a complete set of trace elements, for which reason only a reduced number of samples appear in some graphs.

Whole-rock composition for Chichuj samples vary from andesite to dacite (Fig. 2.7a) with 59–63 wt% SiO_2 (Mora et al. 2004); while Tacaná shows a wider compositional range varying from basaltic andesite to dacite with 54–63 wt% SiO_2 (Macías et al. 2000; Mora et al. 2004; Arce et al. 2008), (Fig. 2.7a). One whole-rock chemical analysis for Las Ardillas Dome (García-Palomo et al. 2006) gave an andesitic composition (63 wt% SiO_2). San Antonio volcano has been sampled extensively, and a robust chemical data set has been published (Macías et al. 2000; Mora et al. 2004; Arce et al. 2014). Its products display a wider compositional range from basaltic andesite to dacite (53–64 wt% SiO_2; Fig. 2.7a). The three pumice-rich pyroclastic deposits (SP, TP, and LVPF), represent the most mafic products reported so far for the TVC (Fig. 2.7a), however, the mafic samples commonly show high loss on ignition values (5–6 wt%), suggesting the occurrence of alteration processes (Arce et al. 2008). A couple of mafic enclaves have been found in San Antonio and Tacaná lavas, and they show a compositional range from basalt to basaltic andesite (51–62 wt% SiO_2; Fig. 2.7a) (Macías et al. 2000; Mora et al. 2004).

As a whole, TVC samples exhibit a wide compositional range from basalt to dacite (49–63 wt% SiO_2, Fig. 2.7a), based on the classification scheme of Le Bas et al. (1986), with the majority lying in the andesitic field. Some of the basaltic samples (SP and TP samples) have unusually low contents of CaO, and high in Al_2O_3 (Figs. 2.7b–j and 2.8a), which likely result from a sericitic alteration (Arce et al. 2012). The Tacaná basalts (including mafic enclaves) are generally less rich in MgO than those from El Chichón (i.e. Chapultenango trachybasalt and mafic enclaves) (Fig. 2.7f). The large-ion-lithophile element concentrations of the Tacaná volcanic rocks are also consistently lower than those from El Chichón (Arce et al. 2014). Some compositional trends of the Tacaná samples on the Harker diagrams are similar to those displayed at El Chichón (i.e. P_2O_5, Fe_2O_3, Ba, K_2O, and K_2O/P_2O_5 ratio), possibly indicating analogous fractionating assemblages and conditions (Fig. 2.7b–j). Notably, the TVC rocks extend to higher K_2O/P_2O_5 than those from El Chichón (Fig. 2.7i). Also, four of the Tacaná basalts (corresponding to mafic enclaves) have somewhat higher TiO_2, but, unlike high-Ti samples from El Chichón, show no other compositional distinctions on Harker diagrams (Fig. 2.7b–j). The overall abundances of the highly and moderately incompatible elements are lower in Tacaná volcanic rocks relative to those from El Chichón (Fig. 2.8). The Tacaná rocks show negative Nb, Ta, and Ti anomalies that differ in general from those of El Chichón rocks, with the exception of the strong positive Pb anomaly (Fig. 2.8). A total of six Nd and Sr isotopic ratios for the TVC have been published (Mora et al. 2004). $^{87}Sr/^{86}Sr$ ratios vary from 0.70441 to 0.70459 whereas $^{143}Nd/^{144}Nd$ ranges from 0.51275 to 0.51282. Despite the few data, all values are similar to those obtained for El Chichón but displaced to higher $^{87}Sr/^{86}Sr$ (Fig. 2.5). These results could indicate a more extensive crustal contamination compared to El Chichón samples, however more isotopic analysis from the TVC are needed to confirm this hypothesis.

2.3 Magma Genesis and Evolution

2.3.1 El Chichón

El Chichón is characterized by eruptions of potassium, sulphur, and H_2O-rich magmas (Luhr 2008) that have been referred to as shoshonitic arc-related magmatism. Even if the content in incompatible elements seems to be inconsistent with a simple subduction zone

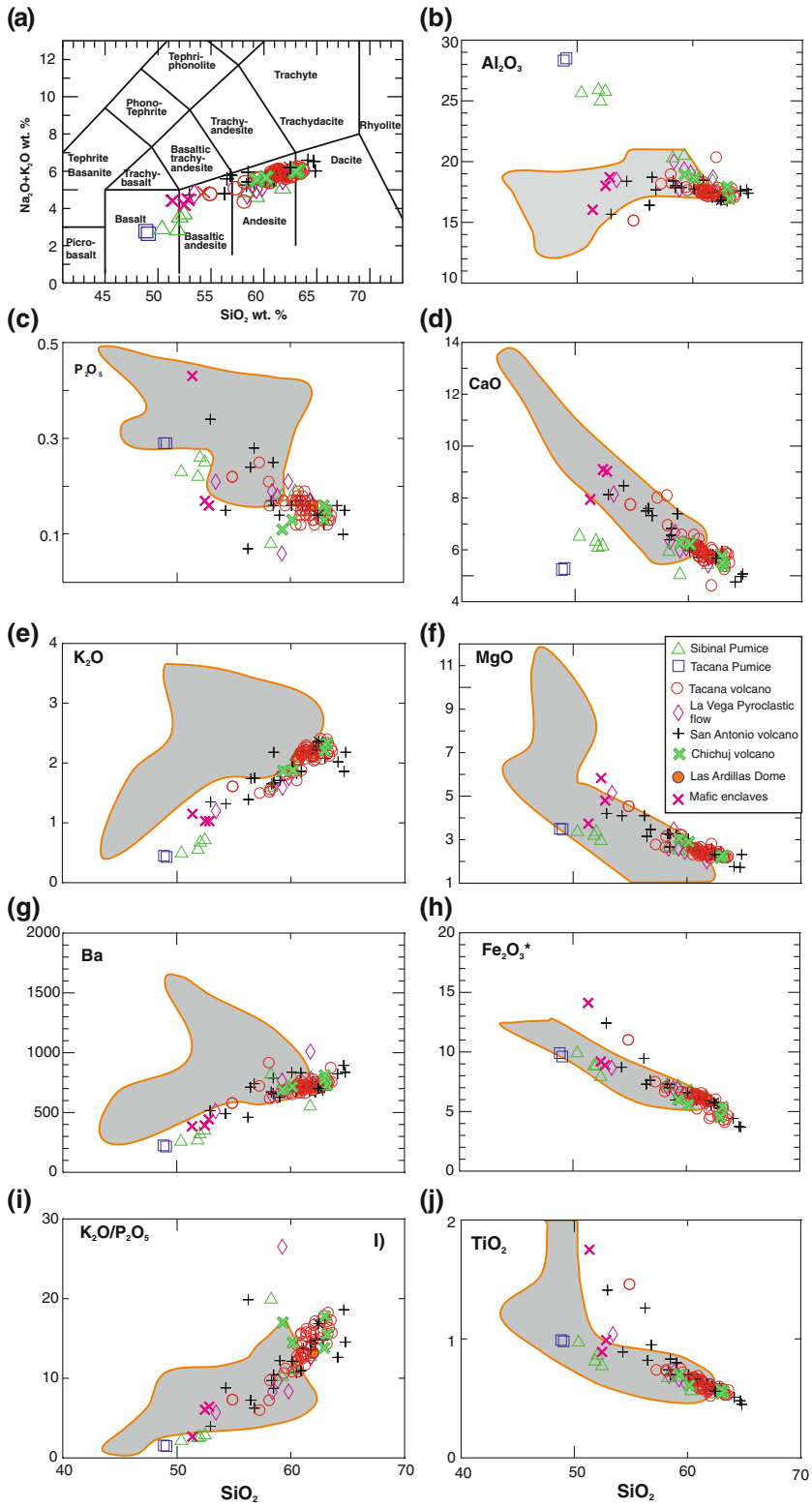

Fig. 2.7 **a** Total alkali versus silica diagram (Le Bas et al. 1986), for Tacaná samples; **b–j** Harker diagrams. Major elements in wt%, and trace elements in ppm. For all samples, major elements were recalculated to 100 % on an anhydrous basis. The *gray* field represents data of El Chichón samples. Data were taken from Macías et al. (2000), Mora et al. (2004), García-Palomo et al. (2006), Macías et al. (2010b), Arce et al. (2012) and Arce et al. (2014)

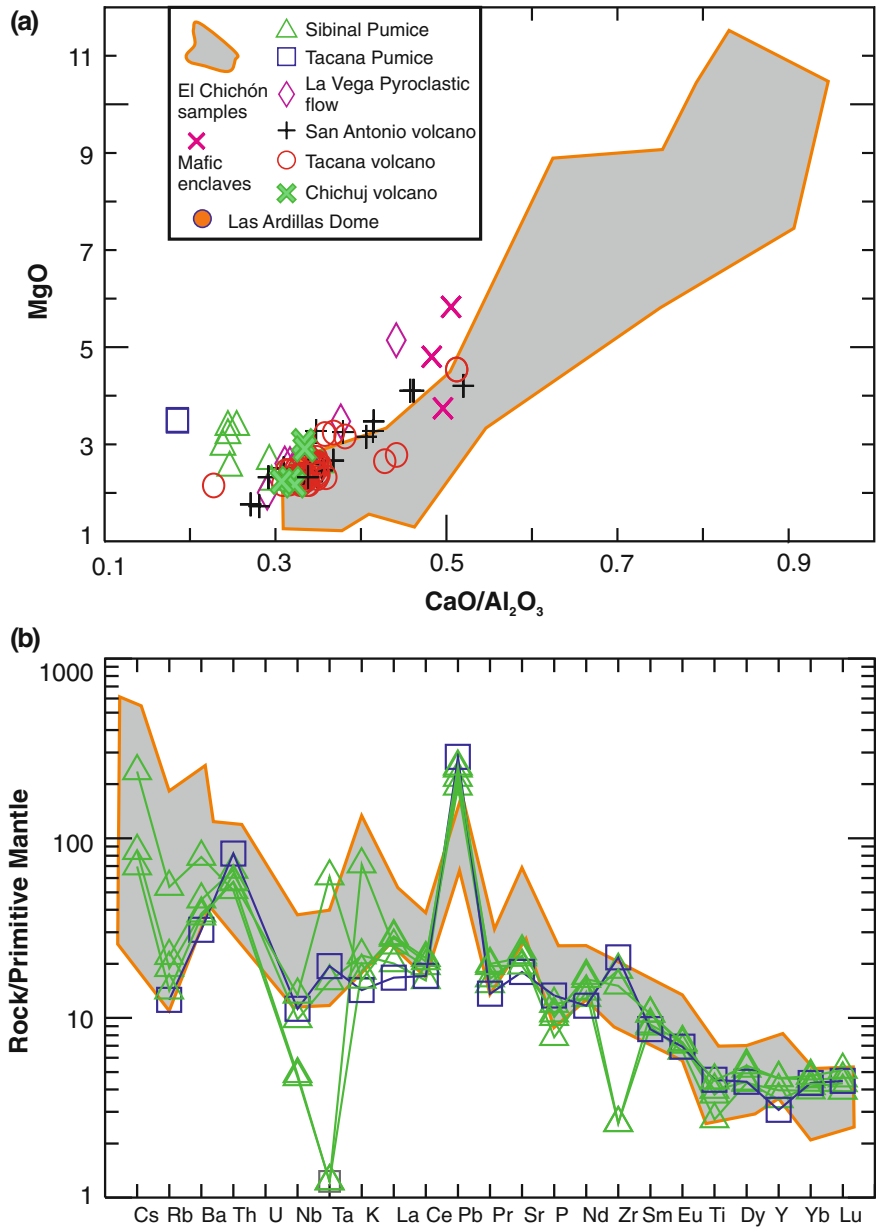

Fig. 2.8 **a** MgO versus CaO/Al_2O_3 ratio for Tacaná samples. All samples were recalculated to 100 % on an anhydrous basis; **b** Spider diagram of selected Tacaná samples normalized to primitive mantle (Sun and McDonough 1989). Note the two samples showing lower values in Ta, Nb, and Zr

signature, the high water contents, and estimated magmatic $\delta^{34}S$ in 1982 eruption products are consistent with a subduction zone provenance (Luhr and Logan 2002; Walker et al. 2003). The strong enrichment in potassium (i.e. Fig. 2.3i) of all products is not well understood. Manea and Manea (2008) attributed the relatively high water contents of El Chichón magmas to the dehydration of a serpentinized oceanic lithosphere, associated with subduction of the Tehuantepec Ridge. This ridge would be highly fractured, and therefore susceptible to deep and pervasive serpentinization.

The geochemistry and mineralogical characteristics of El Chichón rocks, make a difficult task to explain the magma genesis for this volcano. De Ignacio et al. (2003) proposed the presence of adakite-like (high Sr/Y ratios of about 204) that would be produced by melting of the subducted Cocos plate, however only two samples have low Y values (one sample from Unit B and another one for Unit D; see Chap. 6). Although

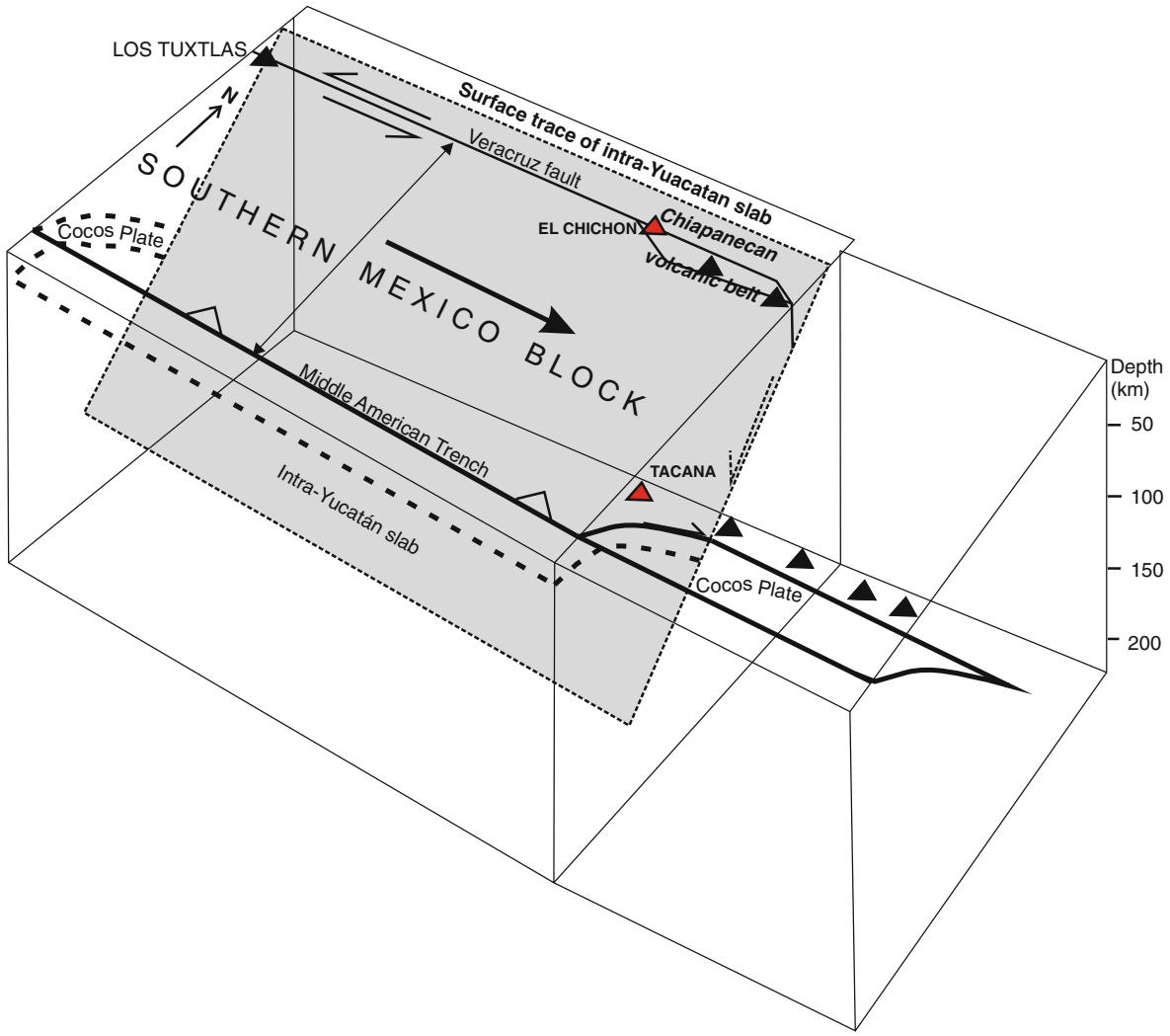

Fig. 2.9 3D tectonic model for southern Mexico involving two subducted slabs (*Cocos* and *Yucatan*). Sinistral movements of the Veracruz fault induces a pull-apart system at the Chiapanecan Volcanic Belt (after Arce et al. 2014)

later, a more robust geochemical data for Unit B demonstrated that Sr/Y ratios are around 50 (Macías et al. 2003), that correspond to mantle melts.

An alternative explanation for the genesis of El Chichón magmas rich in potassium, sulfur, and phosphorous, could be considering such melts as the product of a "rifting" mechanism combined with melting or dehydration of the Yucatan slab (Arce et al. 2014). The Yucatan slab is an oceanic plate dipping to the SW, subducted during the Miocene (Kim et al. 2011) (Fig. 2.9), which could have provided abundant hydrothermal sulfides to the mantle wedge (Arce et al. 2014). The high contents in Ti (>1 wt%) in the magmas of Central American volcanoes have been attributed to melting due to decompression of an asthenospheric mantle (Bolge et al. 2009). This concept could be applied also for El Chichón magmatism, where extensional tectonism has been documented (García-Palomo et al. 2004; Chap. 1). A Cocos-related origin for magmatism at El Chichón is under discussion, considering a truncation of the Cocos Plate at a depth of 100 km by the subducted Yucatán Plate suggested recently by Kim et al. (2011).

The possible rift origin for El Chichón magmas would be in agreement with the lateral movements of the San Juan, Arroyo de Cal, and Caimba faults

(García-Palomo et al. 2004; Chap. 1) that combined with other faults (i.e. Chapultenango Fault) would result in a pull-apart system (Arce et al. 2014) related to the major Polochic-Motagua system (Malfait and Dinkelman 1972). An extensional setting would be characterized by strike-slip faults along a pull-apart system, where volcanic structures would be concentrated, as suggested by Aydin and Nur (1982) and tested in several places around the world (i.e. western United States, Israel, Turkey, and Guatemala). The fault systems at El Chichón suggest a similar setting (i.e. pull-apart), in which magmas would be generated and stored underneath the volcano, as proposed by García-Palomo et al. (2004) and Bursik (2009).

El Chichón trachyandesites appear to be fed by parental mafic magmas that are similar in composition to mafic enclaves found in El Chichon's volcanic rocks and similar to the Chapultenango trachybasalt. Differentiation to high K_2O/P_2O_5 ratios (Fig. 2.3i) and the relatively enriched Sr and Nd isotopic ratios compared to most volcanic rocks of the CAVA (Fig. 2.5), suggest that crustal contamination is a significant process in magmatic evolution (Feigenson and Carr 1986; Wendlandt et al. 1995; Walker et al. 1995, 2007; Cameron et al. 2003). This hypothesis is consistent with isotopic data in phenocrysts of El Chichón volcanic rocks, which suggest that crustal assimilation produce the complex zonation of the plagioclase crystals (Tepley et al. 2000; Andrews et al. 2008; Jones et al. 2008). Luhr (2008) suggested that the high SO_2 flux at El Chichón could be explained by a deep (7–9 km) degassing of a H_2O-and S-rich and highly oxidized magma (i.e. Roberge et al. 2009; Christopher et al. 2010). The existence of a deep magma reservoir below El Chichón (Fig. 2.10) would be also suggested by seismic data previous to the 1982 eruption, which indicate a seismic gap at depths between 7 and 13 km below the volcano. Such area could represent a deeper magma chamber (Jimenez et al. 1999; Chap. 5). The high frequency of eruptions during the last 8,000 years (Espíndola et al. 2000) were explained with repeated injections of mafic magma (45–51 wt% SiO_2) from a deep reservoir (13 km) able to reinvigorate sluggish and cooling trachyandesitic magmas (55–61 wt% SiO_2) at shallower depths (7 km). Pre-eruptive temperatures for the 1982 eruption of El Chichón have been estimated in a range of 750–850 ºC with oxygen fugacities above of the Ni-NiO buffer and pressures of 2.6–5 kb (Luhr 1990), whereas a temperature of

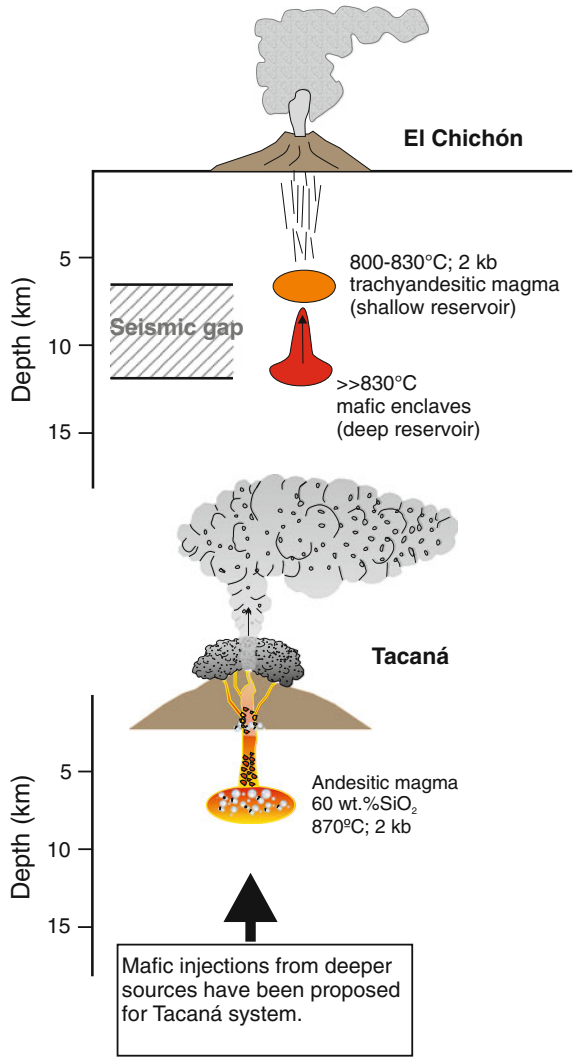

Fig. 2.10 Sketch of El Chichón and Tacaná magmatic systems based on petrologic and seismic data. Temperature and pressure estimates were taken from Luhr (1990); Macías et al. (2003), Arce et al. (2008, 2012)

880 ºC, with oxygen fugacities of −11 and a pressure of 3 kb have been calculated for the eruption occurred ~550 year BP (Unit B, see Chap. 6) (Macías et al. 2003) (Fig. 2.10).

As a whole, the Modern Chiapanecan Volcanic Arc lies along the northeastern border of the Southern Mexico Block proposed by Andreani et al. (2008). In this light, the genesis of the CVA could be related to the ESE movement of the Southern Mexico Block relative to North America (Andreani et al. 2008). Nevertheless, to date, no clear explanations exist,

either for the genesis of trachybasaltic magmas at El Chichón, or for the presence or absence of the Tehuantepec ridge just underneath El Chichón, and its possible role on the genesis of sulphur-potassium-rich magmas. It is urgent to perform more isotopic analyses, and specific studies on trace elements, to better understand the magma genesis at El Chichón and the entire Modern Chiapanecan Volcanic Arc.

2.3.2 Tacaná

Geochemical characteristics of magmas erupted at the TVC are more typical of a subduction-related environment with respect to those of El Chichón, even if much less is known about magma genesis and evolution because of lack of studies. With the available data, magma genesis seems more clearly associated with subduction of the Cocos Plate considering that Tacaná volcanic rocks have distinct Nb, Ta, and Ti anomalies (Arce et al. 2014). The Nb and Ta anomalies seem to be related to fluids from the subducted plate (Wood et al. 1979), because released fluids from the slab contribute to the enrichment of "lithophile" elements in the magmas produced in convergent zones. Nb and Ta are not involved in this enrichment because they are not mobilized by fluids, due to the presence of insoluble phases in the subducting plates, therefore Nb and Ta would be retained in the slab (Saunders et al. 1980). Using the Ba/La ratio as a gauge of slab (fluid) contribution (i.e. Carr et al. 1990), the Tacaná magmas exhibit a slightly higher slab (fluid) signature than those of El Chichón (Fig. 2.11). This would be consistent with the shallow slab depth

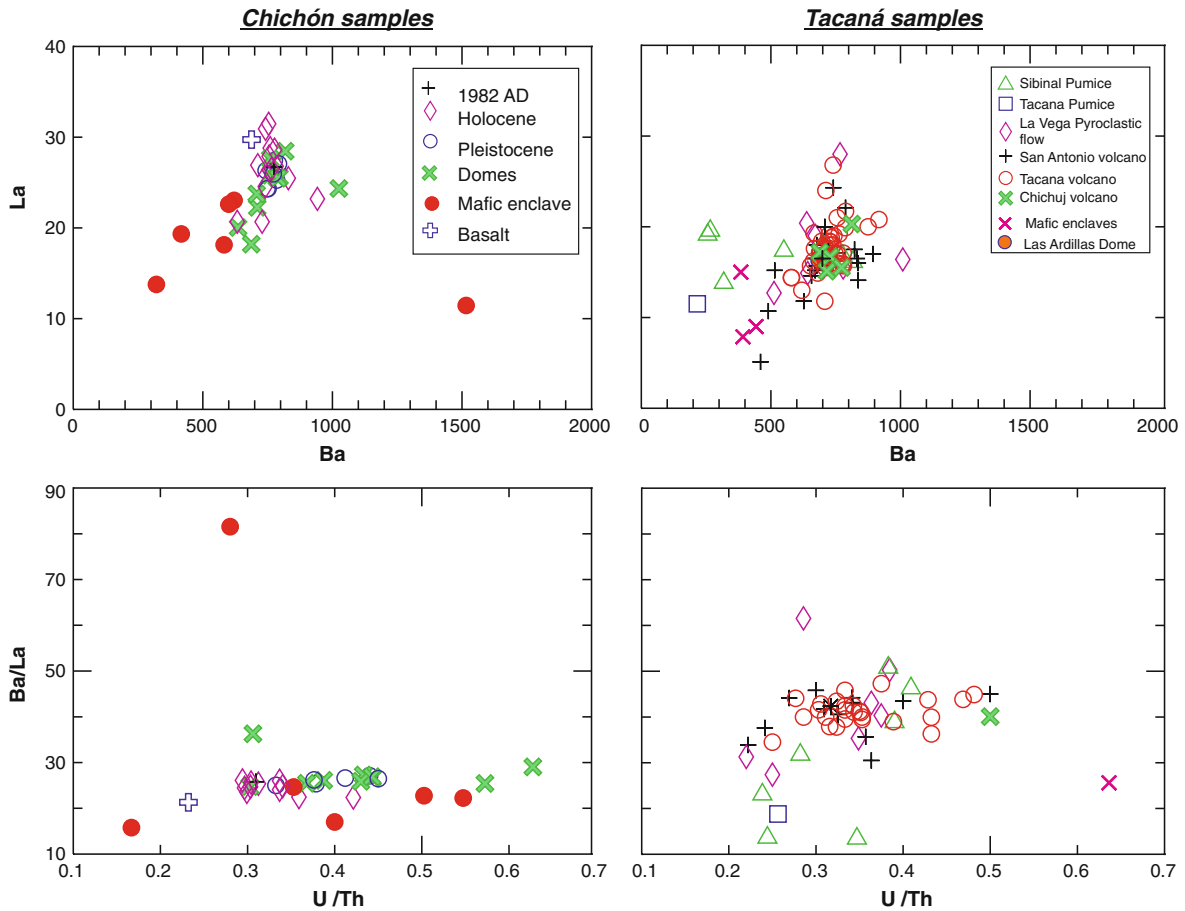

Fig. 2.11 El Chichón and Tacaná samples plotted on Ba versus La and Ba/La versus U/Th diagrams. Notice that the behavior of Tacaná rocks suggests an important slab contribution in generating magmas (Carr et al. 1990). Data from Arce et al. (2014)

beneath Tacaná, as recently proposed by Arce et al. (2014), considering that other studies suggest that slab signatures decrease with increasing slab depth (i.e. Walker et al. 2003). A greater influence of the slab would be also indicated by the higher $^{87}Sr/^{86}Sr$ ratios of the Tacaná volcanic rocks (Fig. 2.5).

Incoming mafic magmas are somewhat heterogeneous considering that a high-Ti component must also be entering the magmatic system (Fig. 2.7j). The common occurrence of amphibole would represent the evidence that Tacaná magmas, like those at El Chichón, were water-rich. As occurs at El Chichón, the relatively enriched Sr and Nd isotope ratios (Fig. 2.5) and evolution to high K_2O/P_2O_5 (Fig. 2.7i) would indicate that crustal contamination plays an important role during magmatic differentiation (Arce et al. 2014). Macías et al. (2000) already emphasized the role of magma mixing for Tacaná products. They proposed that mafic magma (54 wt% SiO_2) entered to an existing magmatic reservoir and mixed with the resident andesitic melt (60–63 wt% SiO_2). Mixing produced the observed mafic enclaves in the Mixcun pyroclastic flow deposit (see Chap. 6). Such mixing event would have been responsible for destabilizing the magmatic system and provoking the eruption ~1950 years before present (Macías et al. 2000).

The intrusion of hot magma and mixing into a cooler reservoir (870 ºC) likely represents the trigger for many of Tacaná's explosive eruptions (Arce et al. 2012) by causing the over pressurization of the magmatic system (i.e. Eichelberger 1995; Sparks et al. 1997). Pre-eruptive temperature estimates for the three pumice-rich pyroclastic deposits (LVPF, SP fallout, and TP fall) range between 870–920 ºC for the La Vega pyroclastic flow, and ca. 890 ºC for the SP and TP fallout deposits (Fig. 2.10; Arce et al. 2008) (see Chap. 6 for stratigraphic details). An on-going petrological experimental study on the San Antonio dacitic dome suggests an equilibration pressure of ~2 kb, which would correspond roughly to depths of 7 km for the magma chamber at the TVC (Fig. 2.10) (Mora et al. 2013).

In summary, both El Chichón and Tacaná, considered subduction-related volcanoes, have emitted distinct types of magmas, one alkaline with anomalous enrichments in potassium, and sulfur (El Chichón), the other more typical calc-alkaline (Tacaná). Both volcanoes have experienced repetitive injections of mafic magmas (indicated by the presence of mafic enclaves) that have mixed in crustal magma chambers and triggered explosive eruptions. Nevertheless, both volcanoes need more detailed petrologic and geochemical studies in order to understand the genesis of high potassium and sulphur magmas at El Chichón, and the genesis of high-Ti magmas at Tacaná volcano.

References

Abers GA, Plank T, Hacker R (2003) The wet Nicaraguan slab. Geophys Res Lett 30:1098. doi:10.1029/2002GL015649

Andreani L, Rangin C, Martínez-Reyes J, Le Roy C, Aranda-García M, Le Pichon X, Peterson-Rodriguez R (2008) Neogeneleft-lateral shearing along the Veracruz fault: the eastern boundary of the southern Mexico Block. Bull Soc Géol Fr 179:195–208

Andrews BJ, Gardner JE, Housh T (2008) Repeated recharge, assimilation, and hybridization in magmas erupted from El Chichón as recorded by plagioclase and amphibole phenocrysts. J Volc Geotherm Res 175:415–426

Arce JL, Macías JL, Gardner J (2008) The ~14 Ka Plinian-type eruption of Tacaná Volcanic complex, Mexico-Guatemala. Eos Trans AGU 89(53), Fall Meeting Suppl, Abs V11C-2060

Arce JL, Macías JL, Gardner JE, Rangel E (2012) Reconstruction of the Sibinal Pumice, an andesitic Plinian eruption at Tacaná Volcanic complex, México-Guatemala. J Volc Geotherm Res 217–218:39–55

Arce JL, Walker J, Keppie JD (2014) Petrology of two contrasting Mexican volcanoes, the Chiapanecan (El Chichón) and Central American (Tacaná) volcanic belts: the result of rift- versus subduction-related volcanism. Int Geol Rev 56:501–524

Aydin A, Nur A (1982) Evolution of pull-apart basin and their scale independence. Tectonics 1:91–105

Best MG (2003) Igneous and metamorphic petrology. Blackwell Publishing, Berlin Germany, p 729

Bolge LL, Carr MJ, Milidakis KI, Lindsay FN, Feigenson M (2009) Correlating geochemistry, tectonics, and volcanic volume along the Central American volcanic front. Geochem Geophys Geosyst 10:1–15

Browne B, Gardner JE (2006) The influence of magma ascent path on the texture, mineralogy, and formation of horblende reaction rims. Earth Planet Sci Lett 246:161–176

Browne BL, Eichelberger JC, Patino LC, Vogel TA, Uto K, Hoshizumi H (2006) Magma mingling as indicated by texture and Sr/Ba ratios of plagioclase phenocrysts from Unzen volcano, SW Japan. J Volc Geotherm Res 154:103–116

Bursik M (2009) A general model for tectonic control of magmatism: examples from Long Valley Caldera (USA) and El Chichón (Mexico). Geof Int 48:171–183

Cameron BI, Walker JA, Carr MJ, Patino LC, Matias O, Feigenson MD (2003) Flux versus decompression melting at stratovolcanoes in southeastern Guatemala. J Volc Geotherm Res 119:21–50

Carr MJ, Feigenson MD, Bennett E (1990) Incompatible element and isotopic evidence for tectonic control of source mixing and melt extraction along the Central American arc. Contrib Mineral Petrol 105:369–380

Carr MJ, Feigenson MD, Patino LC, Walker JA (2003) Volcanism and geochemistry in Central America: progress and problems. In: Eiler (ed) Inside the subduction factory. Geophys Mon Ser 138:153–179

Christopher T, Edmonds M, Humphreys MCS, Herd R (2010) Volcanic gas emissions from Soufrière Hills Volcano, Montserrat 1995–2009, with implications for mafic magma supply and degassing. Geophys Res Lett 37. doi:10.1029/2009GL041325

Damon P, Montesinos E (1978) Late Cenozoic volcanism and metallogenesis over an active Benioff Zone in Chiapas, Mexico. Ar Geol Soc Dig 11:155–168

De Ignacio C, Castiñeiras P, Márquez A, Oyarzun R, Lillo J, López I (2003) El Chichón volcano (Chiapas Volcanic Belt, Mexico) transition calc-alkaline to adakitic-like magmatism: petrologic and tectonic implications. Int Geol Rev 45:1020–1028

DeLong SE, Hodges FN, Arculus RJ (1975) Ultramafic and mafic inclusions, Kanaga Island, Alaska, and the occurrence of alkaline rocks in island arcs. J Geol 83:721–736

Eichelberger JC (1995) Silicic volcanism: ascent of viscous magmas from crustal reservoirs. Annu Rev Earth Plan Sci 23:41–63

Eichelberger JC, Gooley R, Nitsan U, Rice A (1976) A mixing model for andesitic volcanism (abstract). EOS Trans AGU 57:1024

Espíndola JM, Macías JL, Tilling RI, Sheridan M (2000) Eruptive history of el Chichón volcano (Chiapas, Mexico) and its impact on human activity. Bull Volc 62:90–104

Feigenson MD, Carr M (1986) Positively correlated Nd and Sr isotope ratios of lavas from the Central American volcanic front. Geology 14:79–82

Feigenson MD, Carr M (1993) The source of Central American lavas: Inferences from geochemical inverse modeling. Contrib Mineral Petrol 113:226–235

García-Palomo A, Macías JL, Espíndola JM (2004) Strike-slip faults and K-alkaline volcanism at El Chichón volcano southeastern México. J Volc Geotherm Res 136:247–268

García-Palomo A, Macías JL, Arce JL, Mora JC, Hughes S, Saucedo R, Espíndola, JM, Escobar R, Layer P (2006) Geological evolution of the Tacaná Volcanic complex, México-Guatemala. In: Rose WI (ed) Volcanic Hazards in Central America, Spec Pap Geol Soc Am 412:39–58

Gazel E, Carr M, Hoernle K, Feigenson M, Szymanski D, Hauff F, van den Bogaard P (2009) Galapagos-OIB signature in southern Central America: mantle refertilization by arc-hot spot interaction. Geochem Geophys Geosyst 10:1–32. doi:10.1029/2008GC002246

Guzman-Speziale M, Pennington WD, Matumoto T (1989) The triple junction of the North America, Cocos, and Caribbean Plates: seismicity and tectonics. Tectonics 8:981–999

Jiménez Z, Espíndola VH, Espíndola JM (1999) Evolution of the seismic activity from the 1982 eruption of El Chichón volcano, Chiapas, Mexico. Bull Volc 61:411–422

Jones DA, Layer PW, Newberry RJ (2008) A 3100-year history of argon isotopic and compositional variation at El Chichón volcano. J Volc Geotherm Res 175:427–443

Kim YH, Clayton RW, Keppie F (2011) Evidence of a collision between the Ycatán Block and Mexico in the Miocene. Geophys J Int 187:989–1000

Layer PW, García-Palomo A, Jones D, Macías JL, Arce JL, Mora JC (2009) El Chichón volcanic complex, Chiapas, México: stages of evolution based on field mapping and 40Ar/39Ar geochronology. Geof Int 48:33–54

Le Bas MJ, Le Maitre RW, Streckeisen A, Zanettin R (1986) A chemical classification of volcanic rocks based on the total alkali-silica diagram. J Petrol 27:745–750

Luhr JF (1990) Experimental phase relations of water- and sulfur- saturated arc magmas and the 1982 eruptions of El Chichón volcano. J Petrol 31:1071–1114

Luhr JF (2008) Primary igneous anhydrite: progress since its recognition in the 1982 El Chichón trachyandesite. J Volc Geotherm Res 175:394–407

Luhr JF, Logan MA (2002) Sulfur isotope systematics of the 1982 El Chichón trachyandesite: an ion microprobe study. Geochim Cosmochim Acta 66:3303–3316

Luhr JF, Carmichael ISE, Varekamp J (1984) The 1982 eruptions of El Chichón Volcano, Chiapas, Mexico: mineralogy and petrology of the anhydrite-bearing pumices. J Volc Geotherm Res 23:69–108

Macías JL, Espíndola JM, García-Palomo A, Scott KM, Hughes S, Mora J (2000) Late Holocene Peléan style eruption at Tacaná Volcano, Mexico-Guatemala: Past, present, and future hazards. Geol Soc Am Bull 112:1234–1249

Macías JL, Arce JL, Mora JC, Espíndola JM, Saucedo R, Manetti P (2003) A 550 years old Plinian eruption at El Chichón volcano, Chiapas, Mexico: explosive volcanism linked to reheating of the magma reservoir. J Geophys Res 108(B12):2569

Macías JL, Arce JL, Garduño-Monroy VH, Rouwet D, Taran Y (2010a) Estudio de prospeccion geotermica para evaluar el potencial del volcán Chichónal, Chiapas. Unpublished Report- Contract no 9400047770 IGF-UNAM-CFE

Macías JL, Arce JL, García-Palomo A, Mora JC, Layer PW, Espíndola JM (2010b) Late-Pleistocene flank collapse triggered by dome growth at Tacaná volcano, México-Guatemala, and relationship to the regional stress regime. Bull Volc 72:33–53

Malfait BT, Dinkelman MG (1972) Circum-Caibbean tectonic and igneous activity and the evolution of the Caribbean Plate. Geol Soc Am Bull 34:263–291

Manea VC, Manea M (2006) Origin of the modern Chiapanecan Volcanic arc in southern México inferred from thermal models. In: Rose WI (ed) Volcanic hazards in Central America, Spec Pap Geol Soc Am 412: 27–38

Manea M, Manea VC (2008) On the origin of El Chichón volcano and subduction of Tehuantepec Ridge: a geodynamical perspective. J Volc Geotherm Res 175:459–471

Manea M, Manea VC, Ferrar L, Kostoglodov V, Bandy WL (2005) Structure and origin of the Tehuantepec Ridge. Earth Planet Sci Lett 238:64–77

McGee JJ, Tlling RI, Duffield WA (1987) Petrologic characteristics of the 1982 and pre-1982 eruptive products of El Chichon volcano, Chiapas, Mexico. Geof Int 26:85–108

Mercado R, Rose W (1992) Reconocimiento geológico y evaluación preliminar de peligrosidad del Volcán Tacaná, Guatemala/México. Geof Int 31:205–237

Mora JC, Macías JL, García-Palomo A, Espíndola JM, Manetti P, Vaselli O (2004) Petrology and geochemistry of the Tacaná Volcanic Complex, Mexico-Guatemala: evidence for the last 40,000 year of activity. Geof Int 43:331–359

Mora JC, Jaimes-Viera MC, Garduño-Monroy VH, Layer PW, Pompa-Mera V, Godinez ML (2007) Geology and geochemistry characteristics of the Chiapanecan volcanic arc (central area), Chiapas, Mexico. J Volc Geotherm Res 162:43–72

Mora JC, Layer PW, Jaimes-Viera MC (2010) New 40Ar/39Ar ages from the central part of the Chiapanecan Volcanic Arc, Chiapas, México. Geofis Int 51:39–49

Mora JC, Gardner JE, Macías JL, Meriggi L, Santo AP (2013) Magmatic control son eruption dynamics of the 1950 yr B. P. eruption of San Antonio Volcano, Tacaná Volcanic Complex, Mexico-Guatemala. J Volc Geotherm Res 262:134–152

Patino LC, Carr MJ, Feigenson MD (2000) Local and regional variations in Central American arc lavas controlled by variations in subducted sediment input. Contrib Mineral Petrol 138:265–283

Rebollar CJ, Espíndola VH, Uribe A, Mendoza A, Pérez-Vertti A (1999) Distribution of stress and geometry of the Wadati-Benioff zone under Chiapas, Mexico. Geof Int 38:95–106

Roberge J, Delgado-Granados H, Wallace PJ (2009) Mafic magma recharge supplies high CO_2 and SO_2 gas fluxes from Popocatépetl volcano, Mexico. Geology 37:107–110

Rose WI, Bornhorst TJ, Halsor SP, Capaul WA, Plumley PS, De la Cruz-Reyna S, Mota R (1984) Volcán El Chichón Mexico; pre-1982 S-rich eruptive activity. J Volc Geotherm Res 23:147–167

Saunders AD, Tarney J, Weaver SD (1980) Transversal geochemical variations across the Antarctic Peninsula: implication for the genesis of calc-alkaline magmas. Earth Planet Sci Lett 46:344–360

Schmincke HU (2004) Volcanism. Springer, Heidelberg, p 324

Sparks RSJ, Sigurdsson H, Wilson L (1997) Magma mixing: a mechanism for triggering acid explosive eruptions. Nature 267:315–318

Stimac JA, Pearce TH (1992) Textural evidence of mafic-felsic magma interaction in dacite lavas, Clear Lake, California. Am Mineral 77:795–809

Sun S, McDonough W (1989) Chemical and isotopic systematics of oceanic basalts: implications for mantle compositions and processes. In: Saunders A, Norry M (eds) Magmatism in ocean basins, Spec Pap Geol Soc London 42:313–345

Syracuse EM, Abers GA (2006) Global compilation of variations in slab depth beneath arc volcanoes and implications. Geochem Geophys Geosyst 7:Q05017. doi:10.1029/2005GC001045

Tatsumi Y, Kosigo T (1997) Trace element transport during dehydration processes in the subducted oceanic crust: 2. origin of chemical and physical characteristics in arc magmatism. Earth Planet Sci Lett 148:207–221

Tepley FJ, Davidson JP, Tilling RI, Arth J (2000) Magma mixing, recharge and eruption histories recorded in plagioclase phenocrysts from El Chichón Volcano, Mexico. J Petrol 41:1397–1411

von Huene R, Aubouin J, Azema J, Blackington G, Carter JA, Coulbourn WT, Cowan DS, Curiale JA, Dengo CA, Eaas RW, Harrison W, Hesse R, Hussong DM, Ladd JW, Muzylov N, Shiki T, Thompson PR, Westberg J (1980) Leg 67: the deep sea drilling Project Mid-America Trench transect off Guatemala. Geol Soc Am Bull 91:421–432

Walker JA (1981) Petrogenesis of lavas from cinder cone fields behind the volcanic front of Central America. J Geol 89:721–739

Walker JA, Carr MJ, Patino LC, Johnson CM, Feigenson MD, Ward RL (1995) Abrupt change in magma generation processes across the Central American arc in southeastern Guatemala: flux-dominated melting near the base of the wedge to decompression melting near the top of the wedge. Contrib Mineral Petrol 120:378–390

Walker JA, Roggensack K, Patino LC, Cameron BI, Matias O (2003) The water and trace element contents of melt inclusions across an active subduction zone. Contrib Mineral Petrol 146:62–77

Walker JA, Mickelson JE, Thomas RB, Patino LC, Cameron BI, Carr MJ, Feigenson MD, Edwards RL (2007) U-series disequilibria in Guatemalan lavas, crustal contamination, and implications for magma genesis along the Central American subduction zone. J Geophys Res 112:B06205. doi:10.1029/2006JB004589

Wendlandt RF, Altherr R, Neumann ER, Baldridge WS (1995) Petrology, geochemistry, isotopes in Continental Rifts: evolution, structure, tectonics. In: Olsen KH (ed) Developments in geotectonics 25, Elsevier, pp 47–60

Winter (2001) An introduction to igneous and metamorphic petrology. Prentice Hall, Bergen, p 697

Wood DA, Joron JL, Treuil M, Norry M, Tarney J (1979) Elemental and Sr isotope variations in basic lavas from Iceland and the surrounding ocean floor. the nature of mantle source heterogeneities. Contrib Mineral Petrol 70:319–339

http://www.springer.com/978-3-642-25889-3

Active Volcanoes of Chiapas (Mexico): El Chichón and Tacaná

Scolamacchia, T.; Macías, J.L. (Eds.)

2015, XI, 180 p. 71 illus., 54 illus. in color., Hardcover
ISBN: 978-3-642-25889-3